Heliyon 10 (2024) e35359

Contents lists available at ScienceDirect

Heliyon

journal homepage: www.cell.com/heliyon

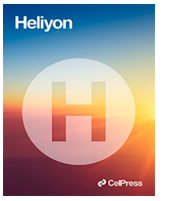

Research article

IGFBP7 mediates oxLDL-induced human vascular endothelial cell injury by suppressing the expression of SIRT1

Jiaju Sun [a], Qingyong Zheng [b], Kaijia Wu [c,*]

[a] Department of Cardiology, Wenzhou Central Hospital, The Dingli Clinical College of Wenzhou Medical University, Wenzhou, China
[b] Infectious Disease Laboratory, Wenzhou Sixth People's Hospital, Wenzhou, China
[c] Electrocardiogram Room, Wenzhou Central Hospital, The Dingli Clinical College of Wenzhou Medical University, Wenzhou, China

ARTICLE INFO

Keywords:
Atherosclerosis
Endothelial dysfunction
IGFBP7
SIRT1

ABSTRACT

Endothelial cell injury plays an important role in initiating atherosclerotic lesion formation. Insulin-like growth factor binding protein 7 (IGFBP7) is known to modulate the behaviors of tumor-associated endothelial cells. This study was conducted to test whether IGFBP7 is involved in endothelial cell injury during atherosclerosis. Oxidized low-density lipoprotein (oxLDL) treatment was used to mimic atherosclerosis-related endothelial cell apoptosis and inflammation response. Small interfering RNA (siRNA) technology was employed to deplete *IGFBP7* expression in human aortic endothelial cells (HAECs). HAECs were exposed to recombinant human IGFBP7 protein to evaluate the function of IGFBP7. Notably, IGFBP7 expression in HAECs was induced by oxLDL treatment. Knockdown of *IGFBP7* or treatment with anti-IGFBP7 abolished oxLDL-induced apoptosis and inflammation in HAECs. Moreover, recombinant IGFBP7 (40 ng/mL but not 25 ng/mL) promoted apoptosis and inflammation in HAECs. IGFBP7 co-localized with CD93 on the surface of HAECs. A mechanistic investigation uncovered that IGFBP7 induced endothelial cell injury through interaction with CD93 and reduction of SIRT1 expression via an autocrine manner. Overexpression of SIRT1 rescued IGFBP7-induced phenotype in HAECs. Taken together, IGFBP7 is induced by oxLDL and mediates oxLDL-induced endothelial cell apoptosis and inflammation, likely through downregulation of SIRT1. These observations support a rationale to prevent atherosclerosis by targeting IGFBP7 activity.

1. Introduction

Endothelial cell dysfunction is a key event during atherosclerotic lesion formation and progression [1]. Oxidized low-density lipoprotein (oxLDL) is recognized as a major pathogenetic factor of atherosclerosis, which affects the biology of multiple cell types including macrophages, vascular smooth muscle cells, and endothelial cells [2,3]. It has been reported that oxLDL elicits reactive oxygen species (ROS) production and induces apoptosis and inflammation in endothelial cells [4,5]. Lectin-like oxidized low-density lipoprotein receptor-1 (LOX-1) is a receptor for oxLDL and participates in the pathogenesis of atherosclerosis [6]. However, the

Abbreviations: HAEC, human aortic endothelial cell; IGFBP7, insulin-like growth factor binding protein 7; LOX-1, low-density lipoprotein receptor-1; oxLDL, oxidized low-density lipoprotein; siRNA, small interfering RNA; TUNEL, terminal deoxynucleotidyl transferase-mediated dUTP nick-end labeling.

* Corresponding author.
E-mail address: wukaijia1123@163.com (K. Wu).

https://doi.org/10.1016/j.heliyon.2024.e35359
Received 22 April 2024; Received in revised form 24 July 2024; Accepted 26 July 2024
Available online 26 July 2024

molecular mechanism involved in endothelial cell injury during atherogenesis is not fully clarified.

Insulin-like growth factor binding protein 7 (IGFBP7) belongs to the IGFBP superfamily and is involved in many biological processes including cell proliferation, adhesion, and differentiation [7,8]. Many studies have established a link between IGFBP7 and tumor progression [9,10]. IGFBP7 is increased in tumor-associated endothelial cells, suggesting its role in tumor angiogenesis [11]. As a secreted protein, IGFBP7 has a capacity to bind to insulin growth factor (IGF), thus regulating IGF signaling [12]. Recently, it has been reported that serum IGFBP7 levels are increased in patients with coronary artery disease compared with healthy volunteers [13]. These findings encourage us to hypothesize that IGFBP7 might participate in the regulation of endothelial cell biology during atherosclerosis.

To test this hypothesis, we employed a model of oxidized low-density lipoprotein (oxLDL)-induced endothelial cell injury and investigated the role of IGFBP7 in this cell model. Our results indicate the involvement of IGFBP7 in oxLDL-induced endothelial cell apoptosis and inflammation. We further explored the mechanism of IGFBP7 action in regulating endothelial cell biology.

2. Materials and methods

2.1. Cell culture and treatment

Primary human aortic endothelial cells (HAECs) were obtained from Lonza (Walkersville, MD, USA) and cultured in Endothelial Cell Growth Medium (Lonza) supplemented with 10 % fetal bovine serum (FBS; Sigma, St. Louis, MO, USA). In this study, HAECs were used at passages 4–8. For oxLDL treatment, HAECs were exposed to 50–150 μg/mL oxLDL (Biosynthesis Biotechnology Company, Beijing, China) for 24 h, as described previously [14]. For IGFBP7 treatment, HAECs were exposed to recombinant human IGFBP7 (13100-H02H; Sino Biological, Beijing, China) at 25 or 40 ng/mL for 24 h. In some experiments, HAECs were treated with anti-IGFBP7 (PA5-102670, ThermoFisher Scientific, Waltham, MA, USA) or anti-CD93 antibody (PA5-52664, ThermoFisher Scientific) at a final concentration of 20 μg/mL for 24 h.

2.2. Plasmids and small interfering RNAs (siRNAs)

Human *SIRT1* cDNA (GenBank accession number: NM_012238) was cloned to pcDNA3.1(+) vector. Specific siRNAs targeting *IGFBP7* (IGFBP7 siRNA#1: 5′-AAGGACAUCUGGAAUGUCATT-3′; IGFBP7 siRNA#2: 5′-CCUCUAAGUAAGGAAGAUGTT-3′) and *CD93* (CD93 siRNA#1: 5′-CUGCCGCUGAAGGGCUUCATT-3′; CD93 siRNA#2: 5′-GGAAAAGGUGAGUUGCUCATT-3′) were synthesized and employed in knockdown experiments.

2.3. Cell transfection

HAECs were seeded into 6-well plates and grew to near 75 % confluence. The cells were transfected with negative control siRNA (siNC) or siRNAs to *IGFBP7* or *CD93* mRNA at a concentration of 40 nM using Lipofectamine RNAiMAX (ThermoFisher Scientific). For overexpression of SIRT1, the pcDNA3.1/SIRT1 plasmid was transfected into HAECs using Lipofectamine 3000 (ThermoFisher Scientific). Twenty-four hours later, the transfected cells were treated with oxLDL (150 μg/mL) or IGFBP7 protein (40 ng/mL) for another 24 h before viability and gene expression analyses.

2.4. RNA isolation and quantitative real-time PCR analysis

Total RNA was purified using TRIzol (ThermoFisher Scientific) and reverse transcribed to cDNA using the SuperScript IV VILO Master Mix (ThermoFisher Scientific). Gene expression was measured by quantitative real time PCR using the Platinum SYBR Green qPCR SuperMix (ThermoFisher Scientific) according to the manufacturer's instructions. The cycling conditions are as follows: 95 °C for 10 min, then 40 cycles of 20 s at 95 °C and 40 s at 60 °C. The gene expression level was normalized to that of *GAPDH* using the $2^{-\Delta\Delta Ct}$ method [15]. PCR primers are shown as follows: *IGFBP7* forward 5′-ACTGGCTGGGTGCTGGTA-3′, *IGFBP7* reverse 5′-TGGATGCATGGCACTCATA-3'; *TNF-α* forward 5′-TGCACTTTGGAGTGATCGGC-3′, *TNF-α* reverse 5′-ACTCGGGGTTCGAGAAGATG-3'; *IL-1β* forward, 5′-ATGCACCTGTACGATCACTGA-3′, *IL-1β* reverse, 5′-ACAAAGGACATGGAGAACACC-3'; *CD93* forward, 5′-GGCAGACAGTTACTCCTGGGT-3′, *CD93* reverse, 5′-GGAGTTCAAAGCTCTGAGGATG-3'; *GAPDH* forward, 5′-GGAGCGAGATCCCTCCAAAAT-3′, *GAPDH* reverse, 5′-GGCTGTTGTCATACTTCTCATGG-3′.

2.5. Western blot analysis

Whole cell lysates were prepared in radioimmunoprecipitation assay (RIPA) buffer containing protease and phosphatase inhibitors (Pierce, Rockford, IL, USA). Protein samples were separated by sodium dodecyl sulfate-polyacrylamide gel electrophoresis. The blots were incubated with primary antibodies (1:500 dilution) overnight at 4 °C, followed by incubation with horseradish peroxidase-conjugated goat anti-rabbit IgG (1:3000 dilution; Santa Cruz Biotechnology, Santa Cruz, CA, USA) for 1 h at room temperature. The primary antibodies used are summarized as follows: anti-IGFBP7 polyclonal antibody (PA5-102670, ThermoFisher Scientific), anti-CD93 polyclonal antibody (PA5-52664, ThermoFisher Scientific), anti-SIRT1 polyclonal antibody (#2310, Cell Signaling Technology, Danvers, MA, USA), and anti-GAPDH monoclonal antibody (#2118, Cell Signaling Technology). The bound immunoproteins were detected using an enhanced chemiluminescent assay (Pierce).

2.6. Enzyme-linked immunosorbent assay (ELISA)

The concentration of IGFBP7 was determined using an ELISA kit (Abcam, Cambridge, MA, USA). After oxLDL treatment, HAECs were cultured under serum-free medium for 24 h before collecting the conditioned medium [16]. Absorbance was recorded at 450 nm using a microplate reader.

2.7. Cell viability assay

Cell viability was measured using the Cell Titer 96 AQueous One Solution Cell Proliferation Assay kit (Promega, Madison, WI, USA). The absorbance of the formazan product was determined at 490 nm, which is proportional to the number of viable cells.

2.8. TUNEL immunofluorescence staining

Cell apoptosis was determined by terminal deoxynucleotidyl transferase (TdT)-mediated dUTP nick-end labeling (TUNEL) staining, as described previously [17]. In brief, HAECs cultured on coverslips were fixed with 4 % paraformaldehyde and permeabilized with 0.3 % Triton X-100 (Sigma). The cells were incubated with the TUNEL reaction mixture (Beyotime Biotechnology, Beijing, China) containing cyanine-3-labeled dUTP in the dark at 37 °C for 1 h. The nuclei were stained with 4′,6-diamidino-2-phenylindole (DAPI). The cells were examined using a fluorescence microscope, and the percentage of TUNEL-positive cells was determined.

2.9. Immunofluorescent staining

HAECs were grown on coverslips, fixed with 4 % paraformaldehyde, and blocked with 4 % bovine serum albumin (Sigma). The cells were incubated with anti-IGFBP7 (PA5-102670, ThermoFisher Scientific; 1:100) and anti-CD93 (14-0939-82, ThermoFisher Scientific; 1:100), followed by incubation with goat anti-rabbit IgG (conjugated with Alexa Fluor 594) or goat anti-mouse IgG (conjugated with Alexa Fluor 488). Nuclei were stained with DAPI. Images were obtained by a fluorescence microscope.

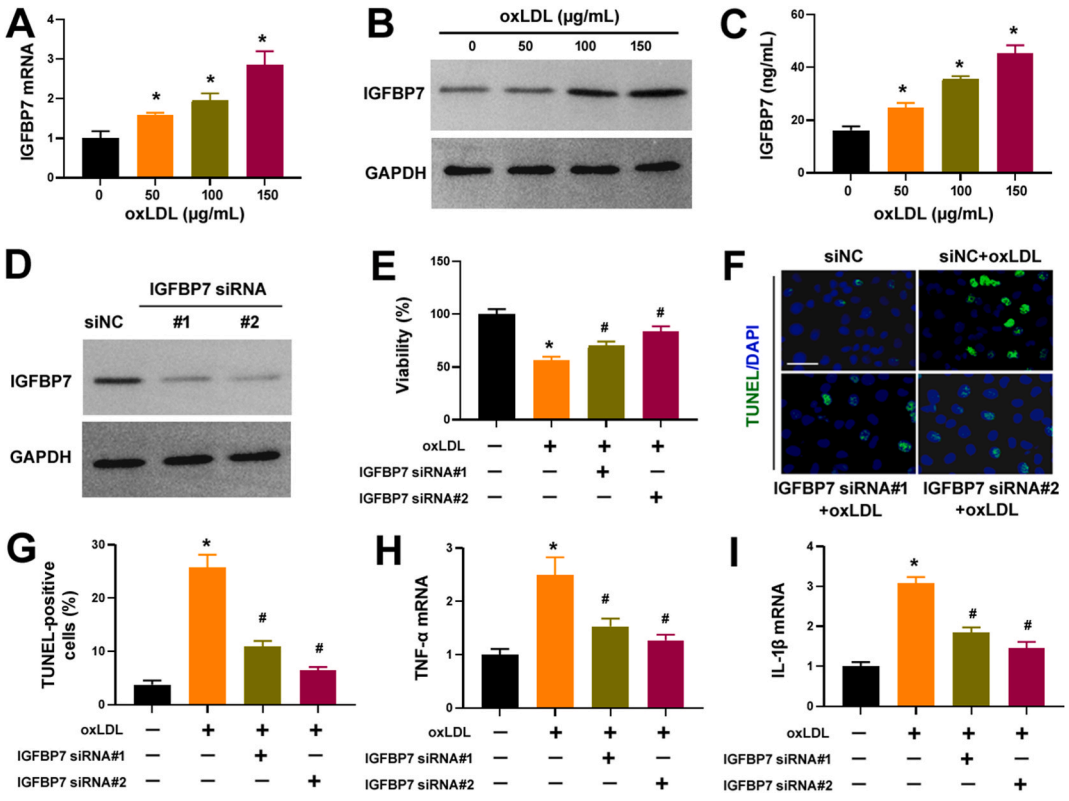

Fig. 1. IGFBP7 depletion blocks oxLDL-induced apoptosis and inflammation in HAECs. (A,B) Analysis of IGFBP7 mRNA (A) and protein (B) in HAECs treated with indicated concentrations of oxLDL. (C) Measurement of IGFBP7 levels in the conditioned medium from HAECs treated with indicated concentrations of oxLDL. *$P < 0.05$ *vs.* untreated control. (D) Analysis of IGFBP7 protein in HAECs transfected with negative control siRNA (siNC) or IGFBP7-targeting siRNAs. *$P < 0.05$ *vs.* the siNC control. (E) Measurement of the viability of HAECs with indicated treatments. (F,G) Apoptosis analysis by TUNEL staining. Scale bar = 50 μm. Quantitative results of TUNEL staining are shown in (F). (H,I) Analysis of TNF-α and IL-1β mRNA levels in HAECs with indicated treatments. *$P < 0.05$ *vs.* untreated control; #$P < 0.05$ *vs.* oxLDL alone.

2.10. Statistical analysis

Data are expressed as mean ± standard deviation. Statistical analysis was performed with one-way analysis of variance (ANOVA) followed by the Tukey's test. $P < 0.05$ was considered significant.

3. Results

3.1. IGFBP7 depletion blocks oxLDL-induced apoptosis and inflammation in HAECs

We first examined the expression of IGFBP7 in the model of oxLDL-induced human vascular endothelial cell injury, which mimics the atheroprone condition. As shown in Fig. 1A and B, oxLDL treatment led to a significant induction of IGFBP7 in HAECs. Moreover,

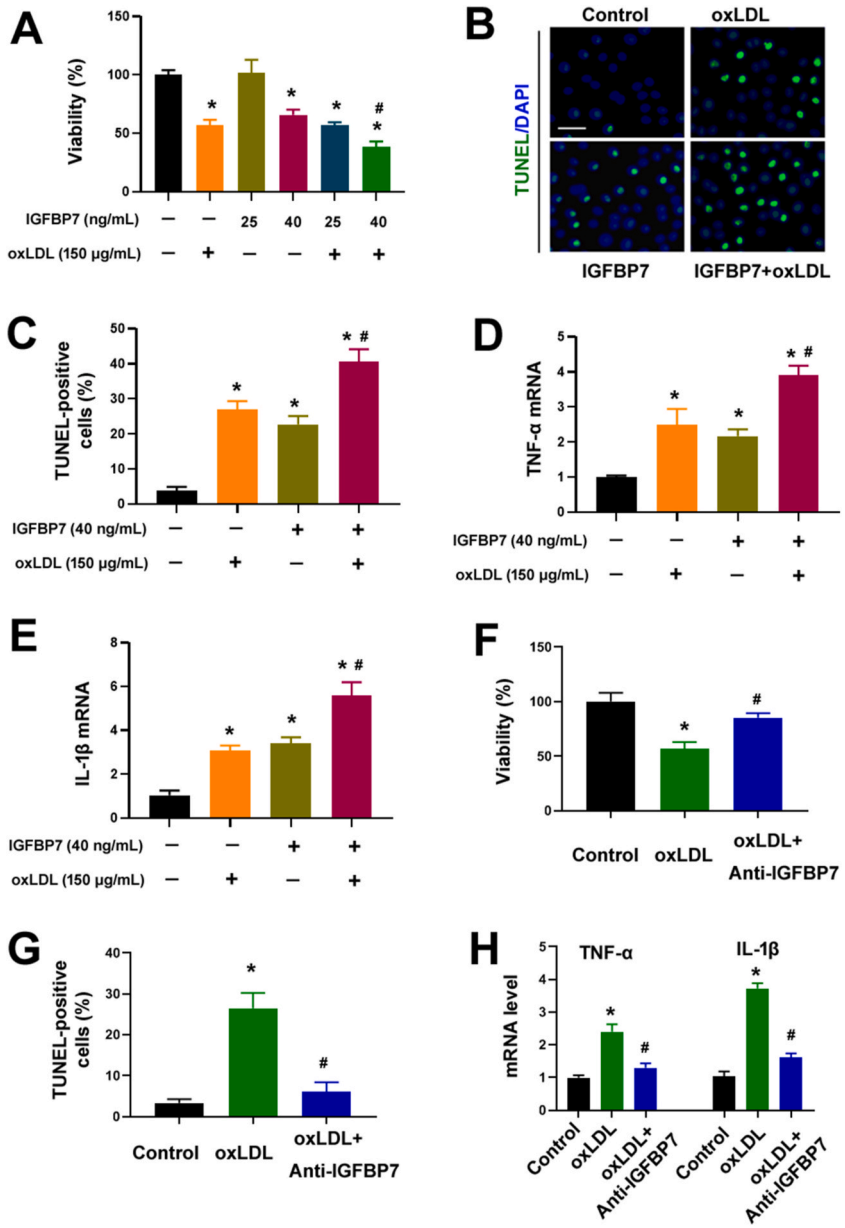

Fig. 2. IGFBP7 aggravates oxLDL-induced vascular endothelial injury. (A) Measurement of the viability of HAECs with indicated treatments. (B,C) Apoptosis analysis by TUNEL staining. Scale bar = 50 μm. Quantitative results of TUNEL staining are shown in (C). (D,E) Analysis of TNF-α and IL-1β mRNA levels in HAECs with indicated treatments. (F) Measurement of the viability of HAECs with indicated treatments. (G) Apoptosis analysis by TUNEL staining. (H) Analysis of TNF-α and IL-1β mRNA levels in HAECs. $^{*}P < 0.05$ *vs.* untreated control; $^{\#}P < 0.05$ *vs.* oxLDL alone.

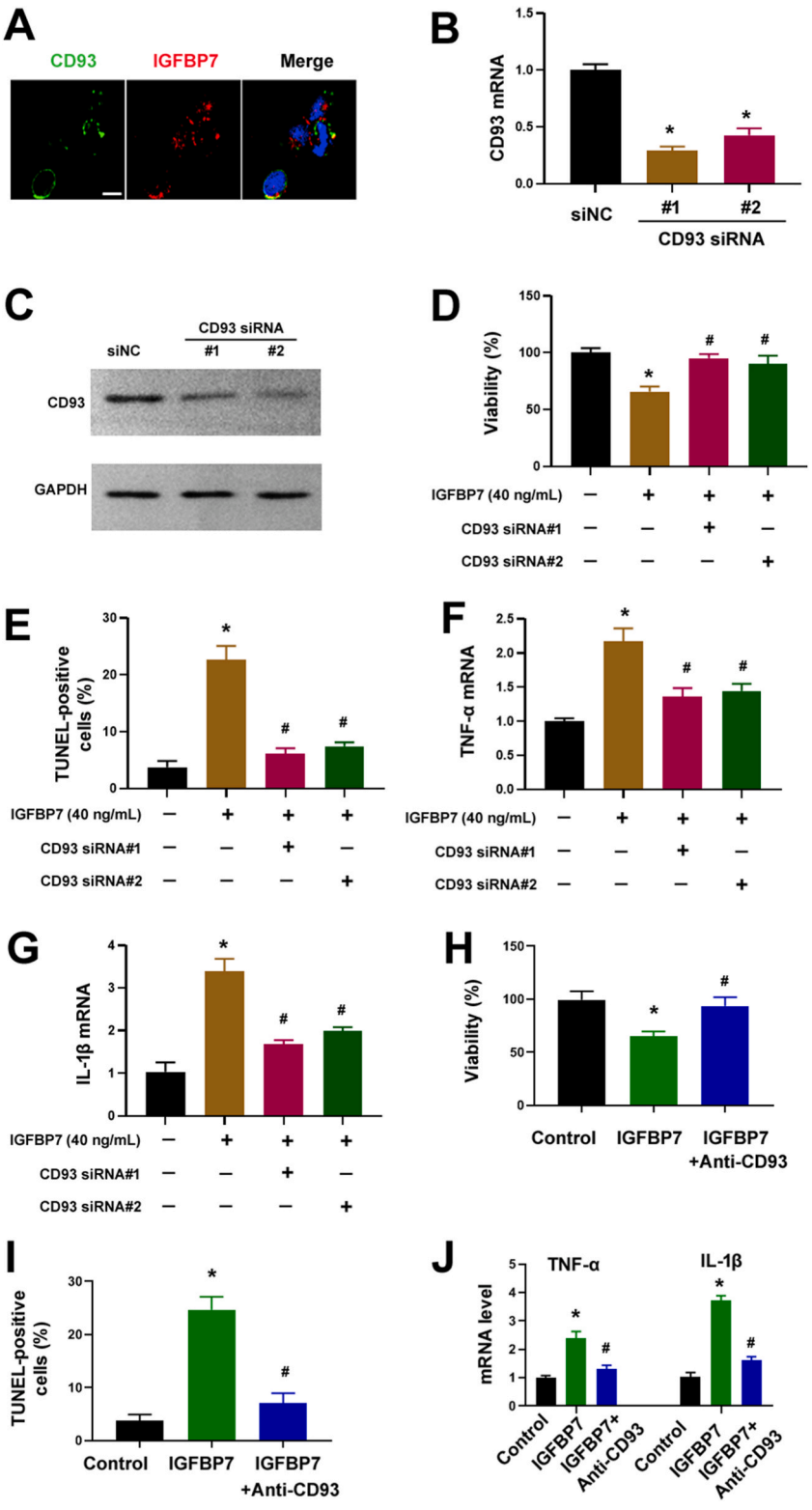

(caption on next page)

Fig. 3. Knockdown of CD93 protects endothelial cells from IGFBP7-induced apoptosis and inflammation. (A) HAECs were co-stained with CD93 (green) and IGFBP7 (red). Scale bar = 20 μm. (B,C) Analysis of CD93 mRNA (B) and protein (C) in HAECs transfected with negative control siRNA (siNC) or CD93-targeting siRNAs. *$P < 0.05$ *vs*. the siNC control. (D) Measurement of the viability of HAECs with indicated treatments. (E) Apoptosis analysis by TUNEL staining. (F,G) Analysis of TNF-α and IL-1β mRNA levels in HAECs with indicated treatments. (H–J) HAECs were treated with 40 ng/mL IGFBP7 in the presence or absence of anti-CD93 antibody. (H) Measurement of cell viability. (I) Apoptosis analysis by TUNEL staining. (J) Analysis of TNF-α and IL-1β mRNA levels in HAECs. *$P < 0.05$ *vs*. untreated control; #$P < 0.05$ *vs*. IGFBP7 alone.

such induction was in a concentration-dependent fashion. ELISA confirmed that the conditioned medium from oxLDL-treated HAECs had a significantly higher concentration of IGFBP7 than control medium (Fig. 1C). These results indicate an induction of IGFBP7 in response to oxLDL treatment.

Next, we interrogated the role of IGFBP7 in oxLDL-induced endothelial cell injury. Two different siRNAs recognizing *IGFBP7* mRNA were employed to knock down the expression of IGFBP7 in HAECs (Fig. 1D). Control siRNA-transfected HAECs displayed a 46 % reduction in viability after exposure to oxLDL (150 μg/mL) for 24 h (Fig. 1E). When *IGFBP7* was silenced by specific siRNAs, oxLDL-induced viability reduction was significantly abolished. The proportion of apoptotic HAECs was significantly increased after treatment with oxLDL (25.8 ± 2.4 % vs. 3.8 ± 0.8 %, $P < 0.05$; Fig. 1F and G). Depletion of *IGFBP7* significantly attenuated oxLDL-induced apoptosis in HAECs. In addition, *IGFBP7* deficiency alleviated oxLDL-induced inflammation response in HAECs, decreasing the expression of inflammatory genes, i.e., TNF-α and IL-1β (Fig. 1H and I). These results suggest that oxLDL-induced vascular endothelial injury may rely on the induction of IGFBP7.

3.2. *IGFBP7 aggravates oxLDL-induced vascular endothelial injury*

IGFBP7 has been identified as a natural ligand for CD93 that is expressed in endothelial cells [11]. Thus, we speculated that IGFBP7 and CD93 might constitute an autocrine loop to directly regulate endothelial cell behaviors. To test this hypothesis, HAECs were

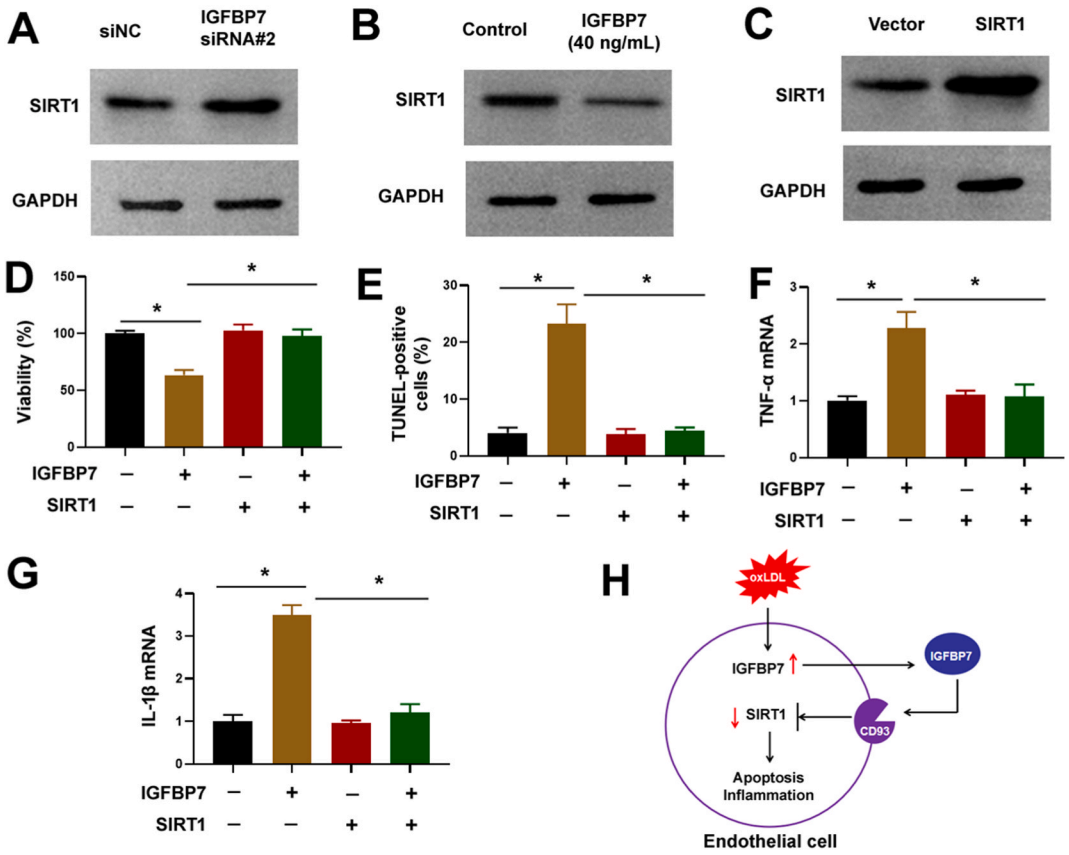

Fig. 4. IGFBP7 promotes endothelial cell apoptosis and inflammation by suppressing the expression of SIRT1. (A) Analysis of SIRT1 protein in HAECs transfected with indicated siRNAs. (B) Analysis of SIRT1 protein in HAECs treated with or without recombinant human IGFBP7 protein. (C) Analysis of SIRT1 protein in HAECs transfected with indicated constructs. (D) Measurement of the viability of HAECs with indicated treatments. (E) Apoptosis analysis by TUNEL staining. (F,G) Analysis of TNF-α and IL-1β mRNA levels in HAECs with indicated treatments. *$P < 0.05$. (H) Proposed mechanism for the role of IGFBP7 in mediating oxLDL-induced vascular endothelial cell injury.

treated with recombinant human IGFBP7 protein at a physiological concentration (25 ng/mL) [13] or greater concentration (40 ng/mL). Recombinant IGFBP7 at 40 ng/mL but not 25 ng/mL significantly decreased the viability of HAECs (Fig. 2A). In the presence of oxLDL, the inhibition of endothelial cell viability was aggravated by 40 ng/mL of IGFBP7. Apoptosis analysis demonstrated that IGFBP7 (40 ng/mL) caused apoptotic death in HAECs, with a marked increase in the apoptotic proportion when combined with oxLDL (Fig. 2B and C). The inflammation response was significantly induced by IGFBP7 (40 ng/mL) alone or in combination with oxLDL (Fig. 2D and E). In addition, blocking IGFBP7 with a specific anti-IGFBP7 antibody significantly reversed oxLDL-induced viability reduction and inflammation in HAECs (Fig. 2F-H). These findings support our hypothesis that IGFBP7 mediates the deleterious effect of oxLDL on endothelial cells.

3.3. Knockdown of CD93 protects endothelial cells from IGFBP7-induced apoptosis and inflammation

Immunofluorescent staining validated that IGFBP7 was colocalized to CD93 on the surface of HAECs (Fig. 3A), suggesting that CD93 is involved in IGFBP7-induced endothelial cell injury. To address this, CD93-targeting siRNAs were transfected to deplete the CD93 expression in HAECs (Fig. 3B and C). IGFBP7-induced viability reduction, apoptosis, and inflammation response were impaired when CD93 was depleted (Fig. 3D-G). Similarly, treatment with anti-CD93 antibody blocked the effects of IGFBP7 on HAECs (Fig. 3H-J). These data suggest that CD93 is indispensable for IGFBP7-induced vascular endothelial cell injury.

3.4. IGFBP7 promotes endothelial cell apoptosis and inflammation by suppressing the expression of SIRT1

Next, we sought to determine how IGFBP7 affects endothelial cell biology. It has been well documented that SIRT1 plays a pivotal role in maintaining endothelial cell viability and function [18,19]. Given that IGFBP7 has the ability to enhance SIRT1 activity in dental pulp-derived mesenchymal stem cells [20], we asked whether IGFBP7-induced endothelial injury is associated with regulation of SIRT1 expression. Of note, knockdown of IGFBP7 increased the expression of SIRT1 in HAECs (Fig. 4A). In contrast, treatment with exogenous IGFBP7 (40 ng/mL) led to a significant reduction of SIRT1 (Fig. 4B). Most importantly, overexpression of SIRT1 rescued IGFBP7-induced endothelial cell apoptosis and inflammation (Fig. 4C-G). Taken together, these results suggest that IGFBP7-mediated vascular endothelial cell injury requires downregulation of SIRT1.

4. Discussion

Given the fact that patients with coronary artery disease have a higher serum IGFBP7 level than healthy volunteers [12], we speculated that upregulation of IGFBP7 might contribute to atherosclerosis-related vascular injury. In support of this hypothesis, our results demonstrate that IGFBP7 is upregulated in HAECs upon exposure to oxLDL. Induction of IGFBP7 is indispensable for oxLDL-induced endothelial cell injury, as evidenced by the fact that knockdown of IGFBP7 ameliorates apoptosis and inflammation in HAECs after oxLDL treatment. Exogenous IGFBP7 at a concentration higher than the physiological level causes damage to HAECs, inducing apoptosis and inflammation. These observations underscore the importance of IGFBP7 in mediating vascular injury during atherogenesis (Fig. 4H).

Upregulation of IGFBP7 occurs in multiple pathological conditions. For example, IGFBP7 levels are high in patients with heart failure and correlate with disease severity [21]. The kidney biopsies from patients with renal disease show greater levels of IGFBP7 than control tissues [22]. IGFBP7 upregulation also predicts the risk of malignant diseases [23,24]. Transforming growth factor beta1 (TGF-β1) is known to promote the expression of IGFBP7 [25]. Alternatively, hypomethylation contributes to the aberrant expression of IGFBP7 in acute leukemia [26]. In this study, we demonstrate that oxLDL treatment induces the expression of IGFBP7 in HAECs. Previous studies have reported that oxLDL induces the activation of TGF-β1 signaling pathway in endothelial cells [27,28]. Therefore, oxLDL-induced IGFBP7 upregulation may be a result of activation of TGF-β1 signaling.

IGFBP7 can be secreted from numerous types of cells such as failing cardiomyocytes [21], renal epithelial cells [25], cancer-associated fibroblasts [23], tumor cells [24], and endothelial cells [29]. Our results confirm that IGFBP7 is released by oxLDL-treated HAECs, which provides an explanation for the high serum IGFBP7 level in patients with coronary artery disease. IGFBP7 has been suggested to exert its biological activity through interaction with CD93, which is a transmembrane glycoprotein mainly expressed on endothelial cells [11,30]. Thus, it is plausible that secreted IGFBP7 could modulate endothelial cell biology via an autocrine fashion. Indeed, our data indicate that IGFBP7 co-localizes with CD93 on the surface of HAECs. Recombinant IGFBP7 protein at a high concentration promotes apoptosis and inflammation in endothelial cells, which resembles the effects of oxLDL on endothelial cells. When recombinant IGFBP7 protein is combined with oxLDL, more robust apoptosis and inflammation response is observed in HAECs. Most importantly, knockdown of CD93 abolishes IGFBP7-induced apoptosis and inflammation in HAECs. These data collectively suggest that IGFBP7 has an autocrine effect on endothelial cells through the CD93-dependent pathway.

A recent study has revealed that the interaction between IGFBP7 and CD93 relies on the IGF-binding domain of IGFBP7 and epidermal growth factor (EGF)-like domain of CD93, with a binding affinity (K_d) of 4.26 μM [31]. However, we demonstrate that IGFBP7 can interact with CD93 in HAECs at a much lower concentration than the *in vitro* Kd value. This may be explained by post-translational modifications of CD93 protein *in vivo*, thus leading to the enhancement of the IGFBP7-CD93 binding. Indeed, it has been documented that CD93 is phosphorylated during endothelial cell adhesion and migration [32].

Our results further reveals that IGFBP7-induced endothelial cell dysfunction is linked to downregulation of SIRT1. SIRT1 is an NAD^+-dependent class III histone deacetylase that is highly expressed in endothelial cells [18,19]. Jiang et al. reported that SIRT1 attenuates IL-1β-induced endothelial cell disruption by deacetylating p66Shc, a redox protein [33]. Activation of SIRT1 protects

endothelial cells from oxLDL-induced inflammation and apoptosis [19]. In dental pulp-derived mesenchymal stem cells, IGFBP7 has been shown to activate SIRT1 [20]. These studies raise the possibility that IGFBP7 might regulate SIRT1 expression in endothelial cells. Unlike the increased SIRT1 activity in IGFBP7-overexpressing mesenchymal stem cells [20], our results indicate that IGFBP7 treatment decreases the expression of SIRT1 in endothelial cells. This discrepancy may originate from different cellular contexts where IGFBP7 modulates SIRT1 expression and activity through cell type-specific factors. Ongoing studies are conducted to clarify the mechanism by which IGFBP7 regulates SIRT1 in endothelial cells. Rescue experiments reveal that overexpression of SIRT1 attenuates IGFBP7-induced endothelial cell injury. Taken together, IGFBP7 exerts its pro-inflammatory and pro-apoptotic activity, at least partially, through downregulation of SIRT1.

Several limitations of this work should be acknowledged. First, there is no evidence for the link between IGFBP7 and SIRT1 expression in atherosclerotic lesions. Second, the potential of targeting IGFBP7 in preventing atherogenesis should be explored in animal models.

In conclusion, IGFBP7 is induced by oxLDL and plays a positive feedback role in oxLDL-induced endothelial cell apoptosis and inflammation. Mechanistically, IGFBP7 negatively regulates the SIRT1 expression, consequently causing endothelial cell injury. Targeting IGFBP7 may represent a potential therapeutic strategy to prevent vascular injury during atherogenesis.

Ethics approval and consent to participate

Not applicable.

Data availability statement

Data will be made available on request.

CRediT authorship contribution statement

Jiaju Sun: Investigation, Data curation, Conceptualization. **Qingyong Zheng:** Software, Methodology, Investigation. **Kaijia Wu:** Writing – review & editing, Writing – original draft, Supervision, Resources, Data curation, Conceptualization.

Declaration of competing interest

All the authors do not have any conflict of interest.

Acknowledgments

This research did not receive any specific grant from funding agencies in the public, commercial, or not-for-profit sectors.

Appendix A. Supplementary data

Supplementary data to this article can be found online at https://doi.org/10.1016/j.heliyon.2024.e35359.

References

[1] C. Wang, C. Liu, J. Shi, H. Li, S. Jiang, P. Zhao, M. Zhang, G. Du, S. Fu, S. Li, Z. Wang, X. Wang, F. Gao, P. Sun, J. Tian, Nicotine exacerbates endothelial dysfunction and drives atherosclerosis via extracellular vesicle-miRNA, Cardiovasc. Res. 119 (2023) 729–742.
[2] T.H. Chiu, C.W. Ku, T.J. Ho, K.L. Tsai, Y.D. Yang, H.C. Ou, H.I. Chen, Schisanhenol ameliorates oxLDL-caused endothelial dysfunction by inhibiting LOX-1 signaling, Environ. Toxicol. 38 (2023) 1589–1596.
[3] Y. He, T. Liu, Oxidized low-density lipoprotein regulates macrophage polarization in atherosclerosis, Int. Immunopharmacol. 120 (2023) 110338.
[4] X. Jin, W. Fu, J. Zhou, N. Shuai, Y. Yang, B. Wang, Oxymatrine attenuates oxidized low-density lipoprotein-induced HUVEC injury by inhibiting NLRP3 inflammasome-mediated pyroptosis via the activation of the SIRT1/Nrf2 signaling pathway, Int. J. Mol. Med. 48 (2021) 187.
[5] Y. Zhao, Y. Li, H. Li, S. Shi, Dopamine D1 receptor activation ameliorates ox-LDL-induced endothelial cell senescence via CREB/Nrf2 pathway, Exp. Cell Res. 425 (2023) 113542.
[6] A.J. Kattoor, A. Goel, J.L. Mehta, LOX-1: regulation, signaling and its role in atherosclerosis, Antioxidants 8 (2019) 218.
[7] J.T. Yu, X.W. Hu, Q. Yang, R.R. Shan, Y. Zhang, Z.H. Dong, H.D. Li, J.N. Wang, C. Li, S.S. Xie, Y.H. Dong, W.J. Ni, L. Jiang, X.Q. Liu, B. Wei, J.G. Wen, M.M. Liu, Q. Chen, Y.R. Yang, G.Y. Zhang, H.M. Zang, J. Jin, Y.G. Wu, X. Zhong, J. Li, W. Wang, X.M. Meng, Insulin-like growth factor binding protein 7 promotes acute kidney injury by alleviating poly ADP ribose polymerase 1 degradation, Kidney Int. 102 (2022) 828–844.
[8] J. Nousbeck, O. Sarig, N. Avidan, M. Indelman, R. Bergman, M. Ramon, C.D. Enk, E. Sprecher, Insulin-like growth factor-binding protein 7 regulates keratinocyte proliferation, differentiation and apoptosis, J. Invest. Dermatol. 130 (2010) 378–387.
[9] D. Li, L. Xia, P. Huang, Z. Wang, Q. Guo, C. Huang, W. Leng, S. Qin, Cancer-associated fibroblast-secreted IGFBP7 promotes gastric cancer by enhancing tumor associated macrophage infiltration via FGF2/FGFR1/PI3K/AKT axis, Cell Death Dis. 9 (2023) 17.
[10] X. Tang, J. Mu, L. Ma, Q. Tan, J. Wang, J. Tan, S. Zhang, IGFBP7 overexpression promotes acquired resistance to AZD9291 in non-small cell lung cancer, Biochem. Biophys. Res. Commun. 571 (2021) 38–45.

[11] Y. Sun, W. Chen, R.J. Torphy, S. Yao, G. Zhu, R. Lin, R. Lugano, E.N. Miller, Y. Fujiwara, L. Bian, L. Zheng, S. Anand, F. Gao, W. Zhang, S.E. Ferrara, A. E. Goodspeed, A. Dimberg, X.J. Wang, B.H. Edil, C.C. Barnett, R.D. Schulick, L. Chen, Y. Zhu, Blockade of the CD93 pathway normalizes tumor vasculature to facilitate drug delivery and immunotherapy, Sci. Transl. Med. 13 (2021) eabc8922.
[12] M. Akiel, C. Guo, X. Li, D. Rajasekaran, R.G. Mendoza, C.L. Robertson, N. Jariwala, F. Yuan, M.A. Subler, J. Windle, D.K. Garcia, Z. Lai, H.H. Chen, Y. Chen, S. Giashuddin, P.B. Fisher, X.Y. Wang, D. Sarkar, IGFBP7 deletion promotes hepatocellular carcinoma, Cancer Res. 77 (2017) 4014–4025.
[13] A. Lisowska, P. Święcki, M. Knapp, M. Gil, W.J. Musiał, K. Kamiński, T. Hirnle, A. Tycińska, Insulin-like growth factor-binding protein 7 (IGFBP 7) as a new biomarker in coronary heart disease, Adv. Med. Sci. 64 (2019) 195–201.
[14] Q. Zeng, J. Xie, F. Li, TRIM59 attenuates ox-LDL-induced endothelial cell inflammation, apoptosis, and monocyte adhesion through AnxA2, Ann. Transl. Med. 11 (2023) 42.
[15] K.J. Livak, T.D. Schmittgen, Analysis of relative gene expression data using real-time quantitative PCR and the 2(-Delta Delta C(T)) Method, Methods 25 (2001) 402–408.
[16] S. Jin, C. Yang, J. Huang, L. Liu, Y. Zhang, S. Li, L. Zhang, Q. Sun, P. Yang, Conditioned medium derived from FGF-2-modified GMSCs enhances migration and angiogenesis of human umbilical vein endothelial cells, Stem Cell Res. Ther. 11 (2020) 68.
[17] K. Zhao, C. Yang, J. Zhang, W. Sun, B. Zhou, X. Kong, J. Shi, METTL3 improves cardiomyocyte proliferation upon myocardial infarction via upregulating miR-17-3p in a DGCR8-dependent manner, Cell Death Dis. 7 (2021) 291.
[18] Z. Wang, M. Zhang, Z. Wang, Z. Guo, Z. Wang, Q. Chen, Cyanidin-3-O-glucoside attenuates endothelial cell dysfunction by modulating miR-204-5p/SIRT1-mediated inflammation and apoptosis, Biofactors 46 (2020) 803–812.
[19] F. Gao, Y. Zhao, B. Zhang, C. Xiao, Z. Sun, Y. Gao, X. Dou, SESN1 attenuates the Ox-LDL-induced inflammation, apoptosis and endothelial-mesenchymal transition of human umbilical vein endothelial cells by regulating AMPK/SIRT1/LOX1 signaling, Mol. Med. Rep. 25 (2022) 161.
[20] X. Li, L. Feng, C. Zhang, J. Wang, S. Wang, L. Hu, Insulin-like growth factor binding proteins 7 prevents dental pulp-derived mesenchymal stem cell senescence via metabolic downregulation of p21, Sci. China Life Sci. 65 (2022) 2218–2232.
[21] T. Ko, S. Nomura, S. Yamada, K. Fujita, T. Fujita, M. Satoh, C. Oka, M. Katoh, M. Ito, M. Katagiri, T. Sassa, B. Zhang, S. Hatsuse, T. Yamada, M. Harada, H. Toko, E. Amiya, M. Hatano, O. Kinoshita, K. Nawata, H. Abe, T. Ushiku, M. Ono, M. Ikeuchi, H. Morita, H. Aburatani, I. Komuro, Cardiac fibroblasts regulate the development of heart failure via Htra3-TGF-β-IGFBP7 axis, Nat. Commun. 13 (2022) 3275.
[22] M. Schanz, M. Kimmel, M.D. Alscher, K. Amann, C. Daniel, TIMP-2 and IGFBP7 in human kidney biopsies in renal disease, Clin. Kidney J. 16 (2023) 1434–1446.
[23] C. Rupp, M. Scherzer, A. Rudisch, C. Unger, C. Haslinger, N. Schweifer, M. Artaker, H. Nivarthi, R. Moriggl, M. Hengstschläger, D. Kerjaschki, W. Sommergruber, H. Dolznig, P. Garin-Chesa, IGFBP7, a novel tumor stroma marker, with growth-promoting effects in colon cancer through a paracrine tumor-stroma interaction, Oncogene 34 (2015) 815–825.
[24] Q. Zhao, R. Zhao, C. Song, H. Wang, J. Rong, F. Wang, L. Yan, Y. Song, Y. Xie, Increased IGFBP7 expression correlates with poor prognosis and immune infiltration in gastric cancer, J. Cancer 12 (2021) 1343–1355.
[25] J. Watanabe, Y. Takiyama, J. Honjyo, Y. Makino, Y. Fujita, M. Tateno, M. Haneda, Role of IGFBP7 in diabetic nephropathy: TGF-β1 induces IGFBP7 via smad2/4 in human renal proximal tubular epithelial cells, PLoS One 11 (2016) e0150897.
[26] S. Heesch, I. Bartram, M. Neumann, J. Reins, M. Mossner, C. Schlee, A. Stroux, T. Haferlach, N. Goekbuget, D. Hoelzer, W.K. Hofmann, E. Thiel, C.D. Baldus, Expression of IGFBP7 in acute leukemia is regulated by DNA methylation, Cancer Sci. 102 (2011) 253–259.
[27] Q. Jin, Y. Deng, L. Li, R. Chen, L. Jiang, miR-19a-3p affected ox-LDL-induced SDC-1/TGF-β1/Smad3 pathway in atherosclerosis, Cell. Mol. Biol. (Noisy-Le-Grand) 69 (2023) 75–81.
[28] Y. Wang, J. Che, H. Zhao, J. Tang, G. Shi, Osthole alleviates oxidized low-density lipoprotein-induced vascular endothelial injury through suppression of transforming growth factor-β1/Smad pathway, Int. Immunopharmacol. 65 (2018) 373–381.
[29] K. Tamura, K. Hashimoto, K. Suzuki, M. Yoshie, M. Kutsukake, T. Sakurai, Insulin-like growth factor binding protein-7 (IGFBP7) blocks vascular endothelial cell growth factor (VEGF)-induced angiogenesis in human vascular endothelial cells, Eur. J. Pharmacol. 610 (2009) 61–67.
[30] G. Tossetta, F. Piani, C. Borghi, D. Marzioni, Role of CD93 in health and disease, Cells 12 (2023) 1778.
[31] Y. Xu, Y. Sun, Y. Zhu, G. Song, Structural insight into CD93 recognition by IGFBP7, Structure 32 (2024) 282–291.
[32] F. Galvagni, F. Nardi, M. Maida, G. Bernardini, S. Vannuccini, F. Petraglia, A. Santucci, M. Orlandini, CD93 and dystroglycan cooperation in human endothelial cell adhesion and migration adhesion and migration, Oncotarget 7 (2016) 10090–10103.
[33] T. Jiang, T. Qin, P. Gao, Z. Tao, X. Wang, M. Wu, J. Gu, B. Chu, Z. Zheng, J. Yi, T. Xu, Y. Huang, H. Liu, S. Zhao, Y. Ren, J. Chen, G. Yin, SIRT1 attenuates blood-spinal cord barrier disruption after spinal cord injury by deacetylating p66Shc, Redox Biol. 60 (2023) 102615.